Preprint typeset in JHEP style - HYPER VERSION

DAMTP-2007-18
Cavendish-HEP-2007-03
MPP-2007-36

Natural Priors, CMSSM Fits and LHC Weather Forecasts

Benjamin C Allanach[1], **Kyle Cranmer**[2], **Christopher G Lester**[3] **and Arne M Weber**[4]

[1] *DAMTP, CMS, Wilberforce Road, Cambridge CB3 0WA, UK*
[1] *Dept. of Physics, New York University, New York, USA*
[3] *Cavendish Laboratory, J.J. Thomson Avenue, Cambridge CB3 0HE, UK*
[4] *Max Planck Inst. für Phys., Föhringer Ring 6, D-80805 Munich, Germany*

Abstract: Previous LHC forecasts for the constrained minimal supersymmetric standard model (CMSSM), based on current astrophysical and laboratory measurements, have used priors that are flat in the parameter $\tan\beta$, while being constrained to postdict the central experimental value of M_Z. We construct a different, new and more natural prior with a measure in μ and B (the more fundamental MSSM parameters from which $\tan\beta$ and M_Z are actually derived). We find that as a consequence this choice leads to a well defined fine-tuning measure in the parameter space. We investigate the effect of such on global CMSSM fits to indirect constraints, providing posterior probability distributions for Large Hadron Collider (LHC) sparticle production cross sections. The change in priors has a significant effect, strongly suppressing the pseudoscalar Higgs boson dark matter annihilation region, and diminishing the probable values of sparticle masses. We also show how to interpret fit information from a Markov Chain Monte Carlo in a frequentist fashion; namely by using the profile likelihood. Bayesian and frequentist interpretations of CMSSM fits are compared and contrasted.

Keywords: Supersymmetry Effective Theories, Cosmology of Theories beyond the Standard Model, Dark Matter.

Contents

1. Introduction

The impending start-up of the LHC makes this a potentially exciting time for supersymmetric (SUSY) phenomenology. Anticipating the arrival of LHC data, a small industry has grown up aiming to forecast the LHC's likely discoveries. There are big differences between nature of the questions answered by a forecast, and the questions that will be answered by the experiments themselves when they have acquired compelling data. A weather forecast predicting "severe rain in Cambridgeshire at the end of the week" should not be confused with a discovery of water. However, the forecast *is* something which influences short-term flood plans and will set priorities within the list of "urgent repairs needed by flood defences".

LHC weather forecasts for sparticle masses or cross sections set priorities among signals needing to be investigated, or among expensive Monte Carlo background samples competing to be generated. Forecasts can influence the design parameters of future experiments and colliders. In advance of LHC we would like to have some sort of idea of what luminosity will be required in order to detect and/or measure supersymmetry. There is also the question of which signatures are likely to be present.

In order to answer questions such as these, a programme of fits to simple SUSY models has proceeded in the literature [4, 5, 6, 7, 8]. The fits that we are interested

in have made the universality assumption on soft SUSY breaking parameters: the scalar masses are set to be equal to m_0, the trilinear scalar couplings are set to be A_0 multiplied by the corresponding Yukawa couplings and all gaugino masses are set to be equal to $M_{1/2}$. Such assumptions, when applied to the MSSM, are typically called mSUGRA or the constrained minimal supersymmetric standard model. The universality conditions are typically imposed at a gauge unification scale $M_{GUT} \sim 2\times 10^{16}$ GeV. The universality conditions are quite strong, but allow phenomenological analysis of a varied subset of MSSM models. The universality assumption is not unmotivated since, for example, several string models [9] predict MSSM universality.

Until recently, CMSSM fits have relied upon fixed input parameters [1, 2, 3, 4, 5, 6, 7] in order to reduce the dimensionality of the CMSSM parameter space, rendering scans viable. Such analyses provide a good idea of what are the relevant physical processes in the various parts of parameter space. More recently, however, it has been realised that many-parameter scans are feasible if one utilises a Markov Chain Monte Carlo (MCMC) [6]. Such scans were used to perform multi-dimensional a Bayesian analysis of indirect constraints [10]. A particularly important constraint came from the relic density of dark matter $\Omega_{DM}h^2$, assumed to consist solely of neutralinos, the lightest of which is the lightest supersymmetric particle (LSP). Under the assumption of a discrete symmetry such as $R-$parity, the LSP is stable and thus still present in the universe after being thermally produced in the big bang. The results of ref. [10] were confirmed by an independent study [11], which also examined the prospects of direct dark matter detection. Since then, a study of the $\mu < 0$ branch of the CMSSM was performed [12] and implications for Tevatron Higgs searches have been discussed [13].

It is inevitable that LHC forecasts will contain a large degree of uncertainty. This is unavoidable as, in the absence of LHC data, constraints are at best indirect and also few in number. Within a Bayesian framework, the components of the answer that are incontestable lie within a simple "likelihood" function, whereas the parts which parameterise our ignorance concerning the nature of the parameter space we are about to explore are rolled up into a prior. By separating components into these two domains, we have an efficient means of testing not only what the data is telling is about new physics, but also of warning us of the degree to which the data is (or isn't) compelling enough to disabuse us of any prior expectations we may hold.

In [10, 11], Bayesian statements were made about the posterior probability density of the CMSSM, after indirect data had been taken into account. The final result of a Bayesian analysis is the posterior probability density function (pdf), which in previous MCMC fits, was set to be

$$p(m_0, M_{1/2}, A_0, \tan\beta, s|\text{data}) = p(\text{data}|m_0, M_{1/2}, A_0, \tan\beta, s)\frac{p(m_0, M_{1/2}, A_0, \tan\beta, s)}{p(\text{data})} \tag{1.1}$$

for certain Standard Model (SM) inputs s and ratio of the two MSSM Higgs vacuum expectation values $\tan\beta = v_2/v_1$. The likelihood $p(\text{data}|m_0, M_{1/2}, A_0, \tan\beta, s)$ is proportional to $e^{-\chi^2/2}$, where χ^2 is the common statistical measure of disagreement between theoretical prediction and empirical measurement. The prior $p(m_0, M_{1/2}, A_0, \tan\beta, s)$ was taken somewhat arbitrarily to be flat (i.e. equal to a constant) within some ranges of the parameters, and zero outside those ranges. Eq. 1.1 has an implied measure for the input parameter. If, for example, we wish to extract the posterior pdf for m_0, all other parameters are marginalised over

$$p(m_0|\text{data}) = \int dM_{1/2}\; dA_0\; d\tan\beta\; ds\; p(m_0, M_{1/2}, A_0, \tan\beta, s|\text{data}). \tag{1.2}$$

Thus a flat prior in, say, $\tan\beta$ also corresponds to a choice of measure in the marginalisation procedure: $\int d\tan\beta$. Before one has a variety of accurate direct data (coming, for instance, from the LHC), the results depend somewhat upon what prior pdf is assumed.

In all of the previous MCMC fits, Higgs potential parameters μ and B were traded for M_Z and $\tan\beta$ using the electroweak symmetry breaking conditions, which are obtained by minimising the MSSM Higgs potential and obtaining the relations [16]:

$$\mu B = \frac{\sin 2\beta}{2}(\bar{m}^2_{H_1} + \bar{m}^2_{H_2} + 2\mu^2), \tag{1.3}$$

$$\mu^2 = \frac{\bar{m}^2_{H_1} - \bar{m}^2_{H_2}\tan^2\beta}{\tan^2\beta - 1} - \frac{M_Z^2}{2}. \tag{1.4}$$

Eqs. 1.3,1.4 were applied at a scale $Q = \sqrt{m_{\tilde{t}_1} m_{\tilde{t}_2}}$, i.e. the geometrical average of the two stop masses[1]. $|\mu|$ was set in order to obtain the empirically measured central value of M_Z in Eq. 1.4 and then Eq. 1.3 was solved for B for a given input value of $\tan\beta$ and $\text{sign}(\mu)$. The flat prior in $\tan\beta$ in Eq. 1.1 does not reflect the fact that $\tan\beta$ (as well as M_Z) is a derived quantity from the more fundamental parameters μ, B. It also does not contain information about regions of fine-tuned parameter space, which we may consider to be less likely than regions which are less fine-tuned. Ref. [15] clearly illustrates that if one includes μ as a fundamental MSSM parameter, LEP has ruled out the majority of the natural region of MSSM parameter space.

A conventional measure of fine-tuning [26] is

$$f = \max_p \left[\frac{d\ln M_Z^2}{d\ln p}\right], \tag{1.5}$$

where the maximisation is over $p \in \{m_0, M_{1/2}, A_0, \mu, B\}$. Here, Eq. 1.4 is viewed as providing a prediction for M_Z given the other MSSM parameters. When the SUSY

[1]Higgs potential loop corrections are taken into account by writing [16] $\bar{m}_{H_i} \equiv m^2_{H_i} - t_i/v_i$, t_i being the tadpoles of Higgs i and v_i being its vacuum expectation value.

parameters are large, a cancellation between various terms in Eq. 1.4 must be present in order to give M_Z at the experimentally measured value. Eq. 1.5 is supposed to provide a measure of how sensitive this cancellation is to the initial parameters. In Ref. [14], a prior $\propto 1/f$ was shown to produce fits that were not wildly different to those with a flat prior, but the discrepancy illustrated the level of uncertainty in the fits. The new (arguably less arbitrary) prior discussed in section 2 will be seen to lead to much larger differences.

Here, we extend the existing literature in two main ways: firstly, we construct a natural prior in the more fundamental parameters μ, B, showing in passing that it can be seen to act as a check on fine-tuning. We display the MCMC fit results from such priors. Secondly, we present posterior pdfs for LHC supersymmetric (SUSY) production cross-sections. These have not been calculated before. We also present a comparison with a more frequentist statistics oriented fit, utilising the profile likelihood. The difference between the flat-priors Bayesian analysis and the profile likelihood contains information about volume effects in the marginalised dimensions of parameter space. We describe an extremely simple and effective way to extract profile likelihood information from the MCMC chains already obtained from the Bayesian analysis with flat priors.

In the proceeding section 2, we derive the new more natural form for the prior distributions mentioned above. In section 3, we describe our calculation of the likelihood. In section 4, we investigate the limits on parameter space and pdfs for sparticle masses resulting from the new more natural priors. We go on to discuss what this prior-dependence means in terms of the "baseline SUSY production" for the LHC, and find out what it tells us about the "error-bars" which should be attached to this and earlier LHC forecasts. In section 5, we present our results in the profile likelihood format. In the following section 6 we present pdfs for total SUSY production cross-sections at the LHC. Section 7 contains a summary and conclusions. In Appendix A, we compare the fit results assuming the flat $\tan\beta$ priors with a well-known result in the literature in order to find the cause of an apparent discrepancy.

2. Prior Distributions

We wish to start with a measure defined in terms of fundamental parameters μ and B, hence

$$p(\text{all data}) = \int d\mu\ dB\ dA_0\ dm_0\ dM_{1/2}\ ds\ \big[p(m_0, M_{1/2}, A_0, \mu, B, s) \\ p(\text{all data}|m_0, M_{1/2}, A_0, \mu, B, s)\big]\,, \tag{2.1}$$

where $p(\text{all data}|m_0, M_{1/2}, A_0, \mu, B, s)$ is the likelihood of the data with respect to the CMSSM and $p(m_0, M_{1/2}, A_0, \mu, B, s)$ is the prior probability distribution for CMSSM and SM parameters. Of these two terms, the former is well defined, while the latter

is open to a degree of interpretation due to the lack of pre-existing constraints on m_0, $M_{1/2}$, A_0, μ, and B[2]. We may approximately factorise the unambiguous likelihood into two independent pieces: one for M_Z and one for other data not including M_Z, the latter defined to be $p(\text{data}|m_0, M_{1/2}, A_0, \mu, B, s)$

$$\begin{aligned} & p(\text{all data}|m_0, M_{1/2}, A_0, \mu, B, s) \\ \approx\ & p(\text{data}|m_0, M_{1/2}, A_0, \mu, B, s) \times p(M_Z|m_0, M_{1/2}, A_0, \mu, B, s) \\ \approx\ & p(\text{data}|m_0, M_{1/2}, A_0, \mu, B, s) \times \delta(M_Z - M_Z^{cen}). \end{aligned} \tag{2.2}$$

In the last step we have approximated the M_Z likelihood by a delta function on the central empirical value M_Z^{cen} because its experimental uncertainties are so tiny. According to the Particle Data Group [17], the current world average measurement is $M_Z = 91.1876 \pm 0.0021$ GeV.

Using Eqs. 1.3,1.4 to calculate a Jacobian factor and substituting Eq. 2.2 into Eq. 2.1, we obtain

$$\begin{aligned} p(\text{all data}) \approx \int & d\tan\beta\ dA_0\ dm_0\ dM_{1/2}\,[r(B, \mu, \tan\beta) \\ & p(\text{data}|m_0, M_{1/2}, A_0, \mu, B, s) p(m_0, M_{1/2}, A_0, \mu, B, s)\big]_{M_Z = M_Z^{cen}}, \end{aligned} \tag{2.3}$$

where the condition $M_Z = M_Z^{cen}$ can be applied by using the constraints of Eqs. 1.3,1.4 with $M_Z = M_Z^{cen}$. The Jacobian factor

$$r(B, \mu, \tan\beta) = M_Z \left| \frac{B}{\mu \tan\beta} \frac{\tan^2\beta - 1}{\tan^2\beta + 1} \right| \tag{2.4}$$

disfavours high values of $\tan\beta$ and μ/B and comes from our more natural initial parameterisation of the Higgs potential parameters in terms of μ, B. We will refer below to $r(B, \mu, \tan\beta)$ in Eq. 2.9 as the "REWSB prior". Note that, if we consider $B \to \tilde{B} \equiv \mu B$ to be more fundamental than the parameter B, one loses the factor of μ in the denominator of r and by sending $\int dB\ d\mu \to \int d\tilde{B}\ d\mu\ \mu$. However, in the present paper we retain B as a fundamental parameter because of its appearance in many supergravity mediation models of SUSY breaking.

It remains for us to define the prior, $p(m_0, M_{1/2}, A_0, \mu, B, s)$, a measure on the parameter space. In our case, this prior must represent our degree of belief in each part of the space, in advance of the arrival of *any* experimental data. There is no single "right" way of representing ignorance in a prior[3], and so some subjectivity

[2]If an earlier experiment had already set clear constraints on m_0, $M_{1/2}$, A_0, μ, B, then even the prior would be well defined, being the result of that previous experiment. As things stand, however, we don't know anything about the likely values of these parameters, and so the prior must encode our ignorance/prejudice as best we can.

[3]There are however plenty of "wrong" ways of representing ignorance. Choosing $p(m_0, M_{1/2}, A_0, \mu, B, s) \propto \delta(m_0 - 40\text{ GeV})(\arctan(A_0/B))^{100}$ would clearly impose arbitrary and unjustifiable constraints on at least three of the parameters!

must enter into our choice. We must do our best to ensure that our prior is as "even handed" as possible. It must give approximately equal measures to regions of parameter space which seem equally plausible. "Even handed" need not mean "flat" however. A prior flat in m_0 is not flat in m_0^2 and very non-flat in $\log m_0$. We must do our best to identify the important (and unimportant) characteristics of each parameter. If the absolute value of a parameter m matters, then flatness in m may be appropriate. If dynamic range in m is more expressive, then flatness in $1/m$ (giving equal weights to each order of magnitude increase in m) may make sense. If only the size of m relative to some related scale M is of importance, then a prior concentrated near the origin in $\log(m/M)$ space may be more appropriate. The freedoms contained within these, to some degree subjective, choices permit others to generate priors different from our own, and thereby test the degree to which the data or the analysis is compelling. If the final results are sensitive to changes of prior, then more data or a better analysis may be called for.

The core idea that we have chosen to encode in (and which therefore defines) our prior on m_0, $M_{1/2}$, A_0, μ, B, and s may be summarised as follows. (1) We define regions of parameter space where there parameters all have similar orders of magnitude to be more natural than those where they are vastly different. For example we regard $m_0 = 10^1$ eV, $M_{1/2} = 10^{20}$ eV as unnatural. In effect, we will use the distance measure between each parameter and a joint 'supersymmetry scale" M_S to define our prior. (2) We do not wish to impose unity of scales at anything stronger than the order of magnitude level. (3) We do not wish to presuppose any particular scale for M_S itself – that is for the data to decide.

Putting these three principles together, we first define a measure that would seem reasonable *were the supersymmetry scale of M_S to be known.* Later we will integrate out this dependence on M_S. To begin with we factorise the prior probability density for a given SUSY breaking scale M_S:

$$\begin{aligned} p(m_0, M_{1/2}, A_0, \mu, B, s|M_S) = p(m_0|M_S)\ p(M_{1/2}|M_S)\ p(A_0|M_S) \\ p(\mu|M_S)\ p(B|M_S)\ p(s), \end{aligned} \tag{2.5}$$

where we have assumed that the SM experimental inputs do not depend upon M_S. This factorisation of priors could be changed to specialise for particular models of SUSY breaking. For example, dilaton domination in heterotic string models predicts $m_0 = M_{1/2} = -A_0/\sqrt{3}$. In that case, one would neglect the separate prior factors for A_0, $M_{1/2}$ and m_0 in Eq. 2.5, leaving only one of them. Since it is our intention to impose unity between m_0, $M_{1/2}$, A_0 and M_S at the "order of magnitude" level, we take a prior probability density

$$p(m_0|M_S) = \frac{1}{\sqrt{2\pi w^2} m_0} \exp\left(-\frac{1}{2w^2}\log^2(\frac{m_0}{M_S})\right). \tag{2.6}$$

The normalising factor in front of the exponential ensures that $\int_0^\infty dm_0\; p(m_0|M_S) = 1$. w specifies the width of the logarithmic exponential, Eq. 2.6 implies that m_0 is within a factor e^w of M_S at the "1σ level" (i.e. with probability 68%). We take analogous forms for $p(M_{1/2}|M_S)$ and $p(\mu\ |M_S)$, by replacing m_0 in Eq. 2.6 with $M_{1/2}$ and $|\mu|$ respectively. Note in particular that our prior $p(\mu|M_S)$ favours superpotential parameter μ to be within an order of magnitude of M_S and thus also within an order of magnitude of the soft breaking parameters. This should be required by whichever model is responsible for solving the μ problem of the MSSM, for example the Giudice-Masiero mechanism [18]. A_0 and B are allowed to have positive or negative signs and values may pass through zero, so we chose a different form to Eq. 2.6 for their prior. However, we still expect that their order of magnitude isn't much greater than M_S and the prior probability density

$$p(A_0|M_S) = \frac{1}{\sqrt{2\pi e^{2w}} M_S} \exp\left(-\frac{1}{2(e^{2w})}\frac{A_0^2}{M_S^2}\right), \tag{2.7}$$

ensures that $|A_0| < e^w M_S$ at the 1σ level. The prior probability density of B is given by Eq. 2.7 with $A_0 \to B$. We don't know M_S a priori, so we marginalise over it:

$$\begin{aligned} p(m_0, M_{1/2}, A_0, \mu, B) &= \int_0^\infty dM_S\; p(m_0, M_{1/2}, A_0, \mu, B|M_S)\; p(M_S) \qquad (2.8)\\ = \frac{1}{(2\pi)^{5/2} w^5 m_0 |\mu| M_{1/2}} &\int_0^\infty \frac{dM_S}{M_S^2} \exp\left[-\frac{1}{2w^2}\left(\log^2(\frac{m_0}{M_S}) + \log^2(\frac{|\mu|}{M_S}) + \right.\right.\\ &\left.\left. \log^2(\frac{M_{1/2}}{M_S}) + \frac{w^2 A_0^2}{e^{2w} M_S^2} + \frac{w^2 B^2}{M_S^2 e^{2w}}\right)\right] p(M_S) \end{aligned}$$

and $p(M_S)$ is a prior for M_S itself, which we take to be $p(M_S) = 1/M_S$, i.e. flat in the logarithm of M_S. The marginalisation over M_S amounts to a marginalisation over a family of prior distributions, and as such constitutes a hierarchical Bayesian approach [19]. The integration over several distributions is equivalent to adding smearing due to our uncertainty in the form of the prior. As far as we are aware, the present paper is the first example of the use of hierarchical Bayesian techniques in particle physics. In general, we could also have marginalised over the hyper-parameter w, for example using a Gaussian centred on 1, but we find it useful below to examine sensitivity of the posterior probability distribution to w. We therefore leave it as an input parameter for the prior distribution. We evaluate the integral in Eq. 2.8 numerically using an integrator that does not evaluate the integrand at the endpoints, where it is not finite. We have checked that the integral is not sensitive to the endpoints chosen: the change induced by changing the integration range to [10 GeV, 10^{16}] GeV is negligible. We refer to Eq. 2.8 as the "same order" prior. To summarise, the posterior probability density function is given by

$$\begin{aligned} p(m_0, M_{1/2}, A_0, \tan\beta, s|\text{data}) \propto \big[&p(\text{data}|m_0, M_{1/2}, A_0, \mu, B, s) \times \qquad (2.9)\\ &r(B, \mu, \tan\beta)\; p(s)\; p(m_0, M_{1/2}, A_0, \mu, B)\big]_{M_Z = M_Z^{cen}}, \end{aligned}$$

where we have written $[\ldots]_{M_Z=M_Z^{cen}}$ on the right hand side of above relation, implying that μ and B are eliminated in favour of $\tan\beta$ and M_Z^{cen} by Eqs. 1.3, 1.4.

We may view the prior factors in Eq. 2.9 to be inverse fine-tuning parameters: where the fine-tuning is high, the priors are small. It is interesting to note that a cancellation of order $\sim 1/\tan\beta$ is known to be required in order to achieve high values of $\tan\beta$ [25]. This appears in our Bayesian prior as a result of transforming from the fundamental Higgs potential parameters μ, B to $\tan\beta$ and the empirically preferred value of M_Z. We display the various prior factors in Fig. 1 as a function of m_0 for all other parameters at the SPS1a CMSSM point [20]: $M_{1/2} = 250$ GeV, $A_0 = 100$ GeV, $\tan\beta = 10$ and all SM input parameters fixed at their central empirical values. The figure displays the REWSB prior, the REWSB prior+same order priors with $w = 1, 2$ (simply marked $w = 1$, $w = 2$ respectively) and the inverse of the fine-tuning parameter defined in Eq. 1.5. We see that the REWSB prior actually increases with m_0 along the chosen line in CMSSM parameter space. This is due to decreasing μ in Eq. 2.4 towards the focus-point[4] at high m_0 [55]. The conventional fine-tuning measure f remains roughly constant as a function of m_0, whereas the same order priors decrease strongly as a function of m_0. This is driven largely by the $1/m_0$ factor in Eq. 2.8 and the mismatch between large m_0 and $M_{1/2} = 250$ GeV, which leads to a stronger suppression for the smaller width $w = 1$ rather than $w = 2$.

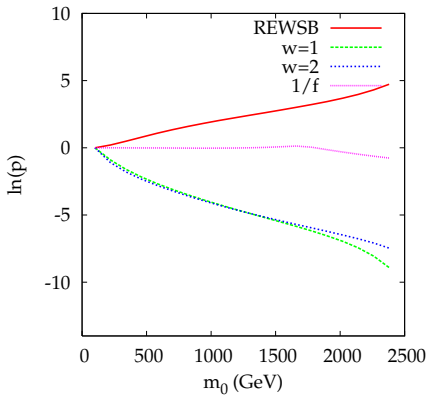

Figure 1: Prior factors p in the CMSSM at SPS1a with varying m_0. Standard Model inputs have been fixed at their empirically central values.

The SM input parameters s used are displayed in Table 1. Since they have all been well measured, their priors are set to be Gaussians with central values and widths as listed in the table. We use Ref. [17] for the QED coupling constant $\alpha^{\overline{MS}}$, the strong coupling constant $\alpha_s^{\overline{MS}}(M_Z)$ and the running mass of the bottom quark $m_b(m_b)^{\overline{MS}}$, all in the $\overline{MS}$ renormalisation scheme. A recent Tevatron top mass m_t measurement [21] is also employed, although the absolutely latest value has shifted slightly [22]. $p(s)$ is set to be a product of Gaussian probability distributions[5] $p(s) \propto \prod_i e^{-\chi_i^2}$, where

$$\chi_i^2 = \frac{(c_i - p_i)^2}{\sigma_i^2} \tag{2.10}$$

for observable i. c_i denotes the central value of the experimental measurement, p_i

[4]The focus-point region is a subset of the hyperbolic branch [53].

[5]Taking the product corresponds to assuming that the measurements are independent.

represents the value of SM input parameter i. Finally σ_i is the standard error of the measurement.

We display marginalised prior pdfs in Fig. 2 for the REWSB, REWSB+same order ($w = 1$) and REWSB+same order ($w = 2$) priors. The plots have 75 bins and the prior pdf has been marginalised over all unseen dimensions. No indirect data has been taken into account in producing the distributions, a feasible electroweak symmetry breaking vacuum being the only constraint. The priors have been obtained by sampling with a MCMC using the Metropolis algorithm [23, 24], taking the average of 10 chains of 100 000 steps each. Figs. 2a,b shows that although the same order priors are heavily peaked towards small values of $m_0 < 500$ GeV and $M_{1/2} \sim 180$ GeV, the 95% upper limits shown by the vertical arrows are only moderately constrained for m_0. $w = 1$ is not surprisingly more peaked at lower mass values. The REWSB histograms on the other hand, prefer high m_0 (due to the lower values of μ there) and are quite flat in $M_{1/2}$. The same order of magnitude requirement is crucial in reducing the preferred scalar masses. The REWSB prior is fairly flat in A_0 whereas the $w = 1$, $w = 2$ priors are heavily peaked around zero. The $M_{1/2}$ same-order priors are more strongly peaked than, for example, m_0 because $M_{1/2}$ is strongly correlated with $|\mu|$ and so the logarithmic measure of the prior (leading to the factor of $1/(m_0 M_{1/2}|\mu|)$ in Eq. 2.8 becomes more strongly suppressed. $\tan\beta$ is peaked very strongly toward lower values of the considered range for the REWSB prior due to the $1/\tan\beta$ suppression, but becomes somewhat diluted when the same order priors are added, as shown in Fig. 2d.

SM parameter	constraint
$1/\alpha^{\overline{MS}}$	127.918±0.018
$\alpha_s^{\overline{MS}}(M_Z)$	0.1176±0.002
$m_b(m_b)^{\overline{MS}}$	4.24±0.11 GeV
m_t	171.4±2.1 GeV

Table 1: SM input parameters

3. The Likelihood

Our calculation of the likelihood closely follows Ref. [14]. For completeness, we describe the procedure here. Including the SM inputs in Table 1, eight input parameters are varied simultaneously. The range of CMSSM parameters considered is shown in Table 2. The SM input parameters are allowed to vary within 4σ of their central values. Experimental errors are so small on the muon decay constant G_μ that we fix it to its central value of 1.16637×10^{-5} GeV^{-2}.

CMSSM parameter	range
A_0	-4 TeV to 4 TeV
m_0	60 GeV to 4 TeV
$M_{1/2}$	60 GeV to 2 TeV
$\tan\beta$	2 to 62

Table 2: Input parameters

In order to calculate predictions for observables from the inputs, the program `SOFTSUSY2.0.10` [27] is first employed to calculate the MSSM spectrum. Bounds upon the sparticle spectrum have been updated and are based upon the bounds

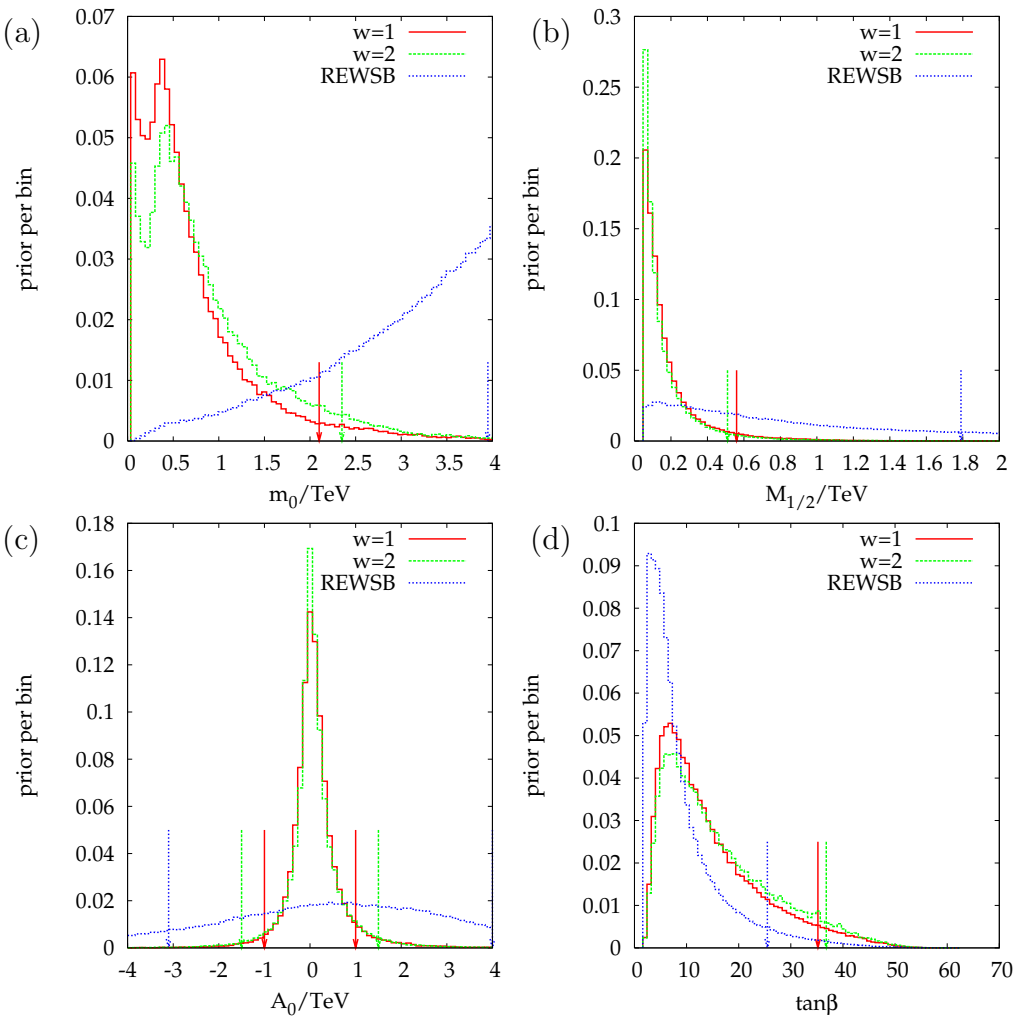

Figure 2: Prior probability distributions marginalised to the (a) m_0, (b) $M_{1/2}$, (c) A_0 and (d) $\tan\beta$ directions. 95% upper limits are shown by the labelled arrows except in (c), where the arrows delimit the 2-sided 95% confidence region. All distributions have been binned with 75 equally spaced bins.

collected in Ref. [11]. Any spectrum violating a 95% limit from negative sparticle searches is assigned a zero likelihood density. Also, we set a zero likelihood for any inconsistent point, e.g. one which does not break electroweak symmetry correctly, or a point that contains tachyonic sparticles. For points that are not ruled out, we then link the MSSM spectrum via the SUSY Les Houches Accord [28] to `micrOMEGAs1.3.6` [29], which then calculates $\Omega_{DM}h^2$, the branching ratios $BR(b \to s\gamma)$ and $BR(B_s \to \mu^+\mu^-)$ and the anomalous magnetic moment of the muon $(g-2)_\mu$.

The anomalous magnetic moment of the muon $a_\mu \equiv (g-2)_\mu/2$ was measured to be $a_\mu^{\rm exp} = (11659208.0 \pm 5.8) \times 10^{-10}$ [30]. Its experimental value is in conflict with the SM predicted value $a_\mu^{\rm SM} = (11659180.4 \pm 5.1) \times 10^{-10}$ from [31], which comprises the latest QED [32], electroweak [33], and hadronic [31] contributions to $a_\mu^{\rm SM}$. This SM prediction however does not account for τ data which is known to lead to significantly

different results for a_μ, implying underlying theoretical difficulties which have not been resolved so far. Restricting to e^+e^- data, hence using the numbers given above, we find

$$\delta\frac{(g-2)_\mu}{2} \equiv \delta a_\mu \equiv a_\mu^{\rm exp} - a_\mu^{\rm SM} = (27.6 \pm 7.7) \times 10^{-10}. \tag{3.1}$$

This excess may be explained by a supersymmetric contribution, the sign of which is identical to the sign of the superpotential μ parameter [34]. After obtaining the one-loop MSSM value of $(g-2)_\mu$ from `micrOMEGAs1.3.6`, we add the dominant 2-loop corrections detailed in Refs. [35, 36]. The W boson mass M_W and the effective leptonic mixing angle $\sin^2\theta_w^l$ are also used in the likelihood. We take the measurements to be [37, 38]

$$M_W = 80.398 \pm 0.027 \text{ GeV}, \qquad \sin^2\theta_w^l = 0.23153 \pm 0.000175, \tag{3.2}$$

where experimental errors and theoretical uncertainties due to missing higher order corrections in SM [39] and MSSM [40, 41] have been added in quadrature. The most up to date MSSM predictions for M_W and $\sin^2\theta_w^l$ [40] are finally used to compute the corresponding likelihoods. A parameterisation of the LEP2 Higgs search likelihood for various Standard Model Higgs masses is utilised, since the lightest Higgs h of the CMSSM is very SM-like once the direct search constraints are taken into account. It is smeared with a 2 GeV assumed theoretical uncertainty in the `SOFTSUSY2.0.10` prediction of m_h as described in Ref. [14]. The rare bottom quark branching ratio to a strange quark and a photon $BR(b \to s\gamma)$ is constrained to be [42]

$$BR(b \to s\gamma) = (3.55 \pm 0.38) \times 10^{-4}, \tag{3.3}$$

obtained by adding the experimental error with the estimated theory error [43] of 0.3×10^{-4} in quadrature. The WMAP3 [44] power law Λ-cold dark matter fitted value of the dark matter relic density is

$$\Omega \equiv \Omega_{DM}h^2 = 0.104^{+0.0073}_{-0.0128} \tag{3.4}$$

In the present paper, we assume that all of the dark matter consists of neutralino lightest supersymmetric particles and we enlarge the errors on $\Omega_{DM}h^2$ to ± 0.02 in order to incorporate an estimate of higher order uncertainties in its prediction.

We assume that the measurements and thus also the likelihoods extracted from Ω, $BR(b \to s\gamma)$, M_W, $\sin^2\theta_w^l$, $(g-2)_\mu$, $BR(B_s \to \mu^+\mu^-)$ are all independent of each other so that the individual likelihood contributions may be multiplied. Observables that have been quoted with uncertainties are assumed to be Gaussian distributed and are characterised by χ^2.

4. CMSSM Fits With the New Priors

In order to sample the posterior probability density, we ran 10 independent MCMCs of 500 000 steps each using a newly developed banked [45] Metropolis-Hastings

MCMC. The banked method was specifically designed to sample several well isolated or disconnected local maxima, for example maxima in the posterior pdfs of $\mu > 0$ and $\mu < 0$. Previously, we had normalised the two samples via bridge sampling [12], which requires twice the number of samples than for one maximum, with additional calculations required after the sampling. Bank sampling, on the other hand, can be performed with roughly an identical number of sampling steps to the case of one maximum and does not require additional normalisation calculations after the sampling. The chance of a bank proposal for the position of the next point in the chain was set to 0.1, meaning that the usual Metropolis proposal had a chance of 0.9. The bank was formed from 10 initial Metropolis MCMC runs with 60 000 steps each and random starting points that were drawn from pdfs flat in the ranges displayed in Tables 1,2. The initial 4000 steps were discarded in order to provide adequate "burn-in" for the MCMCs. We check convergence using the Gelman-Rubin $\hat{R}$ statistic [48, 10], which provides an estimated upper bound on how much the variance in parameters could be decreased by running for more steps in the chains. Thus, values close to 1 show convergence of the chains. In previous publications, we considered $\hat{R} < 1.05$ to indicate convergence of the chains for every input parameter. We have checked that this is easily satisfied for all of our results.

We compare the case of flat $\tan\beta$ priors to the new prior in Fig. 3. The posterior pdf has been marginalised down to the $M_{1/2} - m_0$ plane and binned into 75×75 bins, as with all two-dimensional distributions in the present paper. Both signs of μ have been marginalised over, again like all following figures in this paper unless explicitly mentioned. The bins are normalised with respect to the bin with maximum posterior. We identify the usual CMSSM regions of good-fit in Fig. 3a. The maximum at the lowest value of m_0 corresponds to the stau co-annihilation region [49], where $\tilde{\tau}_1$ and χ_1^0 are quasi-mass degenerate and efficiently annihilate in the early universe. This region is associated with $\tan\beta < 40$, as Fig. 3b indicates. $m_0 \sim 1$ TeV in Fig. 3a has large $\tan\beta \sim 50$. This region corresponds to the case where the neutralinos efficiently annihilate through $s-$channel pseudoscalar Higgs bosons A^0 into $b\bar{b}$ and $\tau\bar{\tau}$ pairs [50, 51]. The region at low $M_{1/2}$ and high m_0 in Fig. 3a is the h^0 pole region [52], where neutralinos annihilate predominantly through an $s-$channel of the lightest CP even Higgs h^0. In order to evade LEP2 Higgs constraints, this also requires large $\tan\beta$. The focus point region [54, 55, 56] is the region around $M_{1/2} \sim 0.5$ TeV and $m_0 = 2 - 4$ TeV, where the lightest neutralino has a significant higgsino component, leading to efficient annihilation into gauge boson pairs. This region is somewhat sub-dominant in the fit, but extends through most of the range of $\tan\beta$ considered.

We see a marked difference between Figs. 3a and 3b. The A^0 and h^0 pole regions have vanished with the REWSB priors. The A^0 pole region is suppressed because the REWSB prior disfavours the required large values of $\tan\beta$, as shown in Fig. 2d. The h^0 pole region is suppressed because the REWSB prior disfavours large values of $|A_0|$,

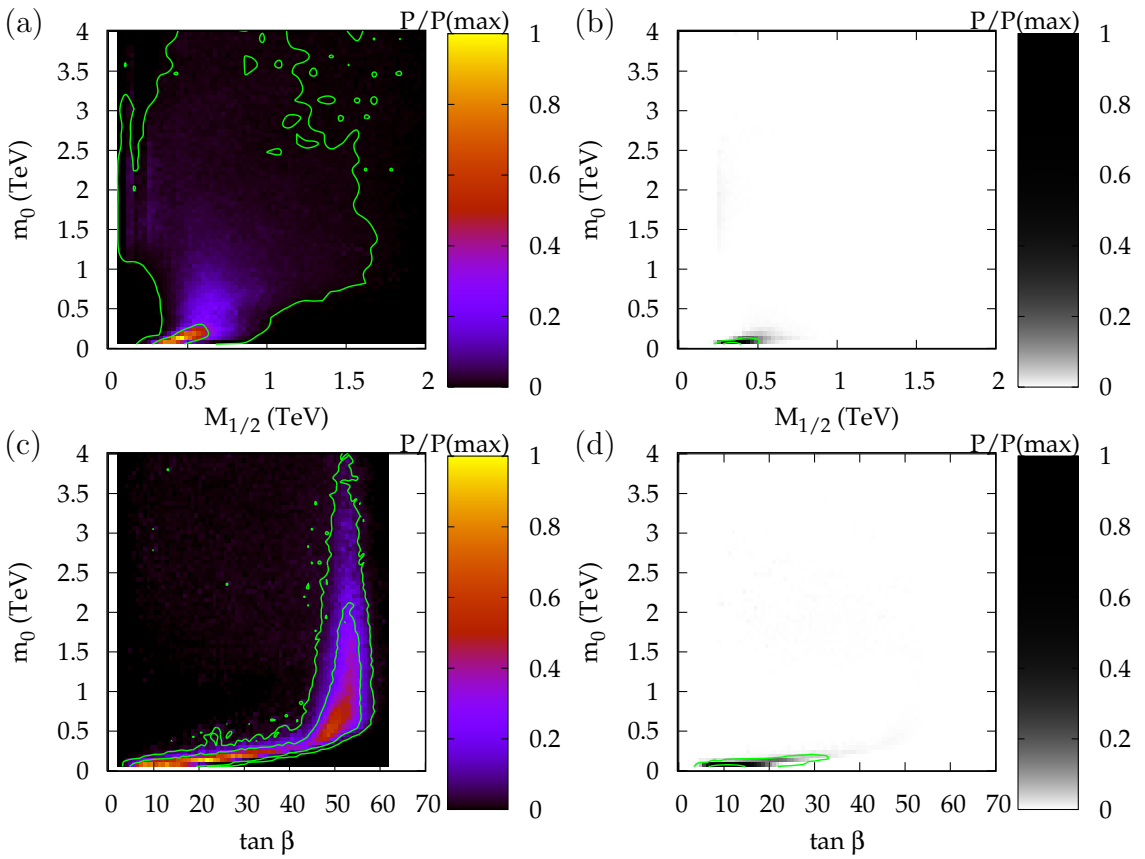

Figure 3: CMSSM fits marginalised in the unseen dimensions for (a,c) flat $\tan\beta$ priors, (b,d) the REWSB+same order prior with $w = 1$. Contours showing the 68% and 95% regions are shown in each case. The posterior probability in each bin, normalised to the probability of the maximum bin, is displayed by reference to the colour bar on the right hand side of each plot.

see Fig. 2c, and large values of $|A_0|/M_{1/2}$. Large values of $|A_0|$ are necessary in this region in order to achieve large stop mass splitting and therefore large corrections to the lightest Higgs mass. Without such corrections, h^0 falls foul of LEP2 Higgs mass bounds. The focus-point region has been diminished by the REWSB priors mainly because the large values of m_0 required become suppressed as in Fig. 2a. This suppression comes primarily from the requirement that SUSY breaking and Higgs parameters be roughly of the same order as each other. Figs. 3b,d display only one good-fit region corresponding to the stau co-annihilation region at low m_0. The banked method [45] allows an efficient normalisation of the $\mu > 0$ and $\mu < 0$ branches, both of which are included in the figure.

We now turn to a comparison of the REWSB+same order prior fits. We consider such fits to give much more reliable results than the flat $\tan\beta$ fits, and a large difference between fits for $w = 1$ to $w = 2$ would provide evidence for a lot of sensitivity

to our exact choice of prior. Some readers might consider the flat $\tan\beta$ priors to be not unreasonable, and those readers could take the large difference between flat priors and the new more natural ones as a result of uncertainty originating from scarce data. Pdfs of sparticle and Higgs masses coming from the fits are displayed

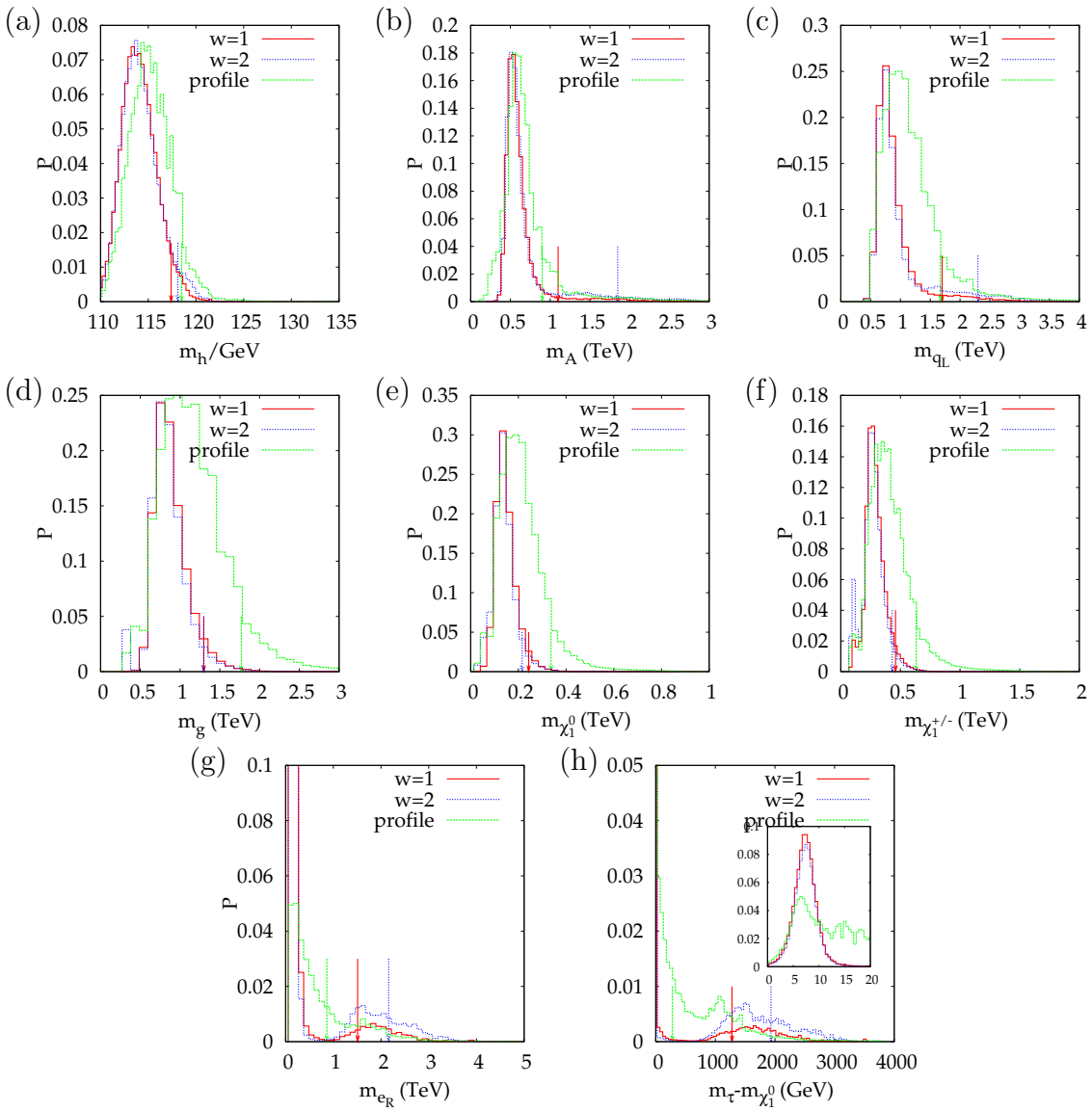

Figure 4: MSSM particle mass pdfs and profile likelihoods: dependence upon the prior in the CMSSM. The vertical arrows display the one-sided 95% upper limits on each mass. There are 75 bins on each abscissa. Histograms marked "profile" are discussed in section 5 and have been multiplied by different dimensionful constants in order to be comparable by eye with the $w = 1, 2$ pdfs. The profile 95% confidence level upper limits are calculated by finding the position for which the 1-dimensional profile likelihood has $2\Delta \ln L = 2.71$ [46].

in Figs. 4a-4h along with 95% upper bounds calculated from the pdfs. The pdfs

displayed are for the masses of (a) the lightest CP even Higgs, (b) the CP-odd Higgs, (c) the left-handed squark, (d) the gluino, (e) the lightest neutralino, (f) the lightest chargino, (g) the right-handed selectron and (h) the lightest-stau lightest-neutralino mass splitting respectively. The most striking feature of the figure is that the Higgs and sparticle masses tend to be very light for the REWSB and same order prior, boding well for future collider sparticle searches. This effect is consistent with a preference for smaller m_0, $M_{1/2}$ exhibited by the new priors in Fig. 2b,d. In general, there is remarkably little difference between the two different cases of $w = 1$ or $w = 2$. This fact is perhaps not so surprising considering that the shape of the priors doesn't change enormously with w, as Figs. 1,2 show. The sparticle mass distributions for priors that are flat in $\tan\beta$ were displayed in Refs. [10, 11, 12] and show a spread up to much higher values of the masses. As we have explained above, we do not believe flat $\tan\beta$ to be an acceptable prior. Some readers may consider it to be so: such readers may consider our fits to be considerably less robust to changes in the prior than Fig. 4 indicates. Lower values of A_0 and $\tan\beta$ help to make the lightest CP-even Higgs light in the REWSB+same order prior case, shown in Fig. 4a. The mass ordering $m_{\tilde{q}_l} > m_{\chi_2^0} > m_{\tilde{l}_R} > m_{\chi_1^0}$ allows a "golden channel" decay chain of $\tilde{q}_l \to \chi_2^0 \to \tilde{l}_R \to m_{\chi_1^0}$. Such a decay chain has been used to provide several important and accurate constraints upon the mass spectrum [60]. In some regions of parameter space, it can also allow spin information on the sparticles involved to be extracted [47]. We may calculate the Bayesian posterior probability of such circumstances by integrating the posterior pdf over the parameter space that allows such a mass ordering. From the MCMC this is simple: we simply count the fraction of sampled points that have such a mass ordering[6]. The posterior probability of such a mass ordering is high: 0.93 for $w = 1$ and 0.85 for $w = 2$, indicating that analyses using the decay chain are likely to be possible (always assuming the CMSSM hypothesis, of course).

As pointed out in Ref. [10], the flat $\tan\beta$ posteriors extend out to the assumed upper range taken on m_0 and so the flat $\tan\beta$ pdf for the scalar masses were artificially cut off at the highest masses displayed. This is no longer the case for the new choice of priors since the regions of large posterior do not reach the chosen ranges of parameters, as shown in Figs. 3b,d. Thus our derived upper bounds on, for instance $m_{\tilde{q}_L}$ in Fig. 4c and $m_{\tilde{e}_R}$ in Fig. 4g are not dependent upon the $m_0 < 4$ TeV range chosen. The mass splitting between the lightest stau and the neutralino is displayed in Fig. 4h. The insert shows a blow-up of the quasi-degenerate stau-co-annihilation region and has a different normalisation to the rest of the plot. Since the REWSB+same order prior fit results lie in the co-annihilation region, nearly all of the probability density predicts that $m_{\tilde{\tau}_1} - m_{\chi_1^0} < 20$ GeV. It is a subject of ongoing research as how to best verify this at the LHC [57]. In Fig. 4g, the plot has been cut

[6]Other absolute probabilities quoted below are calculated in an analogous manner.

off at a probability P of 0.1 and the histograms actually extend to 0.70,0.68 in the lowest bin for $w = 1$ and $w = 2$ respectively. Similarly, we have cut off Fig. 4h at a probability of 0.05. The fits extend to 0.93, 0.85 for $w = 1$, $w = 2$ respectively in the lowest bin.

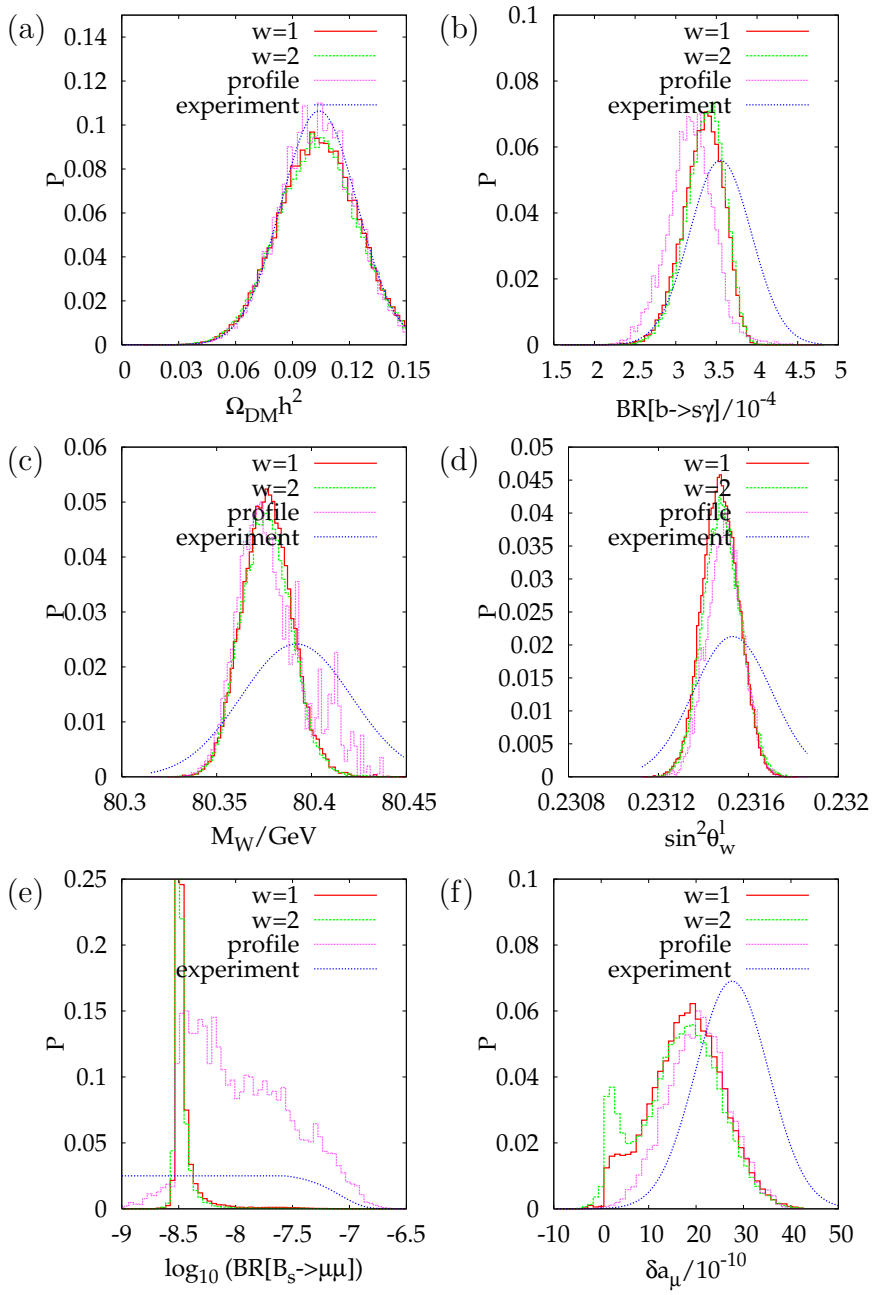

Figure 5: Statistical pull of different observables in CMSSM fits. We show the pdfs for the experimental measurements as well as the posterior pdf of the predicted distribution in $w = 1$ and $w = 2$ fits. Profile histograms are discussed in section 5 and are multiplied by different dimensionful constants in order to be comparable by eye with the $w = 1, 2$ pdfs.

We examine the statistical pull of the various observables in Fig. 5. In each case, the likelihood coming from the empirical constraint is shown by the continuous distribution. The histograms show the fitted posterior pdfs depending upon the prior. We have sometimes slightly altered the normalisation of the curves and histograms to allow for clearer viewing. Fig. 5a shows that the $\Omega_{DM}h^2$ pdf is reproduced well by all fits irrespective of which prior distribution is used. This is because the fits are completely dominated by the $\Omega_{DM}h^2$ contribution, since the CMSSM parameter space typically predicts a much larger value than that observed by WMAP [12]. Figs. 5b,5c,5d show that $BR[b \to s\gamma]$, M_W, $\sin^2\theta_w^l$ are all constrained to be near their central values, with less variance than is required by the empirical constraint. Direct sparticle search limits mean that sparticles cannot be too light and hence cannot contribute strongly to the three observables. The rare decay branching ratio $BR[B_s \to \mu\mu]$ is displayed in Fig. 5e. Both fits are heavily peaked around the SM value of $10^{-8.5}$, indeed the most probable bin has been decapitated in the figure for the purposes of clarity, and really should extend up to a probability of around 0.9. The SUSY contribution to $BR(B_s \to \mu\mu) \propto \tan\beta^6/M_{SUSY}^4$ and so the preference for small $\tan\beta$ beats the preference for smallish sparticle masses $\sim O(M_{SUSY})$ in the new fits. In all of Figs. 5a-e, changing the width of the priors from 1 to 2 has negligible effect on the results. The exception to this trend is δa_μ, as shown in Fig. 5f. δa_μ has a shoulder around zero for $w = 2$, corresponding to a small amount of posterior probability density at high scalar masses, clearly visible from Fig. 4g. Such high masses suppress loops responsible for the SUSY contribution to $(g-2)_\mu$. δa_μ is pulled to lower values than the empirically central value by direct sparticle limits and the preference for values of $\tan\beta$ that are not too large. The almost negligible portion of the graph for which $\delta a_\mu < 0$ corresponds to $\mu < 0$ in the CMSSM. $(g-2)_\mu$ has severely suppressed the likelihood, and therefore the posterior, in this portion of parameter space. For flat $\tan\beta$ priors, and $\delta a_\mu = 22 \pm 10 \times 10^{-10}$, we had previously estimated that the ratio of integrated posterior pdfs between $\mu < 0$ and $\mu > 0$ was $0.7 - 0.16$. For the new priors, where sparticles are forced to be lighter, their larger contribution to δa_μ further suppresses the $\mu < 0$ posterior pdf. From the samples, we estimate[7] $P(\mu < 0)/P(\mu > 0) = 0.001 \pm 002$ for $w = 1$ and 0.003 ± 0.003 for $w = 2$, respectively for $\delta a_\mu = (27.6 \pm 7.7) \times 10^{-10}$. Thus, while the probabilities are not accurately determined, we know that they are small enough to neglect the possibility of $\mu < 0$.

5. Profile Likelihoods

Since, for a flat prior, Eq. 1.1 implies that the posterior is proportional to the likelihood in a Bayesian analysis, one can view the distributions resulting from the MCMC

[7]These numbers come from the mean and standard deviation of 10 chains, each of which is considered to deliver an independent estimate.

scan as being a "likelihood map" [10]. If one marginalises in the unseen dimensions in order to produce a one or two-dimensional plot, one either interprets the resulting distribution probabilistically in terms of the posterior, or alternatively as a way of viewing the full n-dimensional likelihood map, but without a probabilistic interpretation in terms of confidence limits, or credible intervals. Instead, frequentist often eliminate unwanted parameters (nuisance parameters) by maximization instead of marginalization. The likelihood function of the reduced set of parameters with the unwanted parameters at their conditional maximum likelihood estimates is called the profile likelihood [58]. Approximate confidence limits can be set by finding contours of likelihood that differ from the best-fit likelihood by some amount. This amount depends upon the number of "seen dimensions" and the confidence level, just as in a standard χ^2 fit [46].

While we believe that dependence on priors actually tells us something useful about the robustness of the fit, we are also aware that many high energy physicists find the dependence upon a subjective measure distasteful, and would be happier with a frequentist interpretation. When the fits are robust, i.e. there is plentiful accurate data, we expect the Bayesian and frequentist methods to identify similar regions of parameter space in any fits. We are not in such a situation with our CMSSM fits, as we have shown in previous sections, and so we provide the profile likelihood here for completeness.

We can use the scanned information from the MCMC chains to extract the profile likelihood very easily. Let us suppose, for instance, that we wish to extract the profile in $m_0 - M_{1/2}$ space. We therefore bin the chains obtained in $m_0 - M_{1/2}$ as before. We find the maximum likelihood in the chain for each bin and simply plot that. The 95% confidence level region then is delimited by the likelihood contour at a value $2\Delta \ln L = 5.99$ [46], where $\Delta \ln L = \ln L_{max} - \ln L$. The profile likelihoods in the $m_0 - M_{1/2}$ and $m_0 - \tan\beta$ plane are shown in Fig. 6. Comparing Figs. 6a and 3a, we see that the profile likelihood gives similar information to the Bayesian analysis with flat likelihoods. The main difference is that the profile likelihood's confidence limit only extends out to $(M_{1/2}, m_0) < (1.0, 2)$ TeV, whereas for the Bayesian flat-prior analysis, values up to $(M_{1/2}, m_0) < (1.5, 4)$ TeV are viable. Comparing Fig. 6b and 3c, we again see similar constraints, except that the tail at high $\tan\beta$ up to larger values of $m_0 > 2$ TeV has been suppressed in the profile. From the difference we learn the following facts: in this high $\tan\beta$-high m_0 tail, the fit to data is less good than in other regions of parameter space. However, it has a relatively large volume in unseen dimensions of parameter space, which enhances the posterior probability in Fig. 3c. The difference between the two plots is therefore a good measure of such a so-called "volume effect". In ref. [11, 13], an average-χ^2 estimate was constructed in order to identify such effects. We find the profile likelihood to be easier to interpret, however. It also has the added bonus of allowing a frequentist interpretation.

We show the profile likelihoods of the various relevant masses in Fig. 4. There is

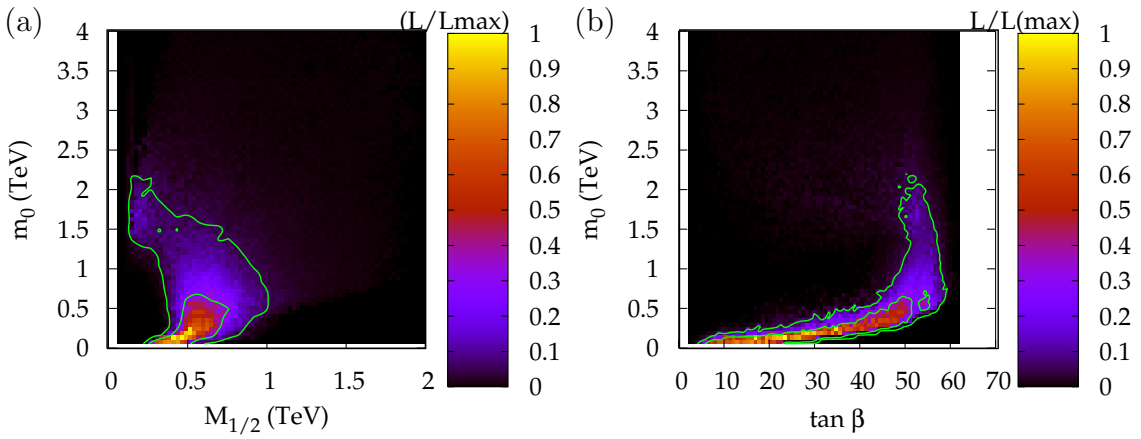

Figure 6: Two dimensional profile likelihoods in the (a) $m_0 - M_{1/2}$ plane, (b) $m_0 - \tan\beta$ plane. There are 75 bins along each direction. The inner (outer) contours show the 68% and 95% confidence level regions respectively.

a general tendency for all of the masses to spread to somewhat heavier values than the $w = 1, 2$ same order+REWSB priors. We remind the reader that the profile likelihood histograms are not pdfs. In the figure, they have been multiplied by dimensionful constants that make them comparable eye to the Bayesian posteriors on the plot. The gluino mass shows the most marked difference: it appears that higher gluino masses are disfavoured by volume effects in the Bayesian analyses. However, while the profiles differ from the Bayesian analyses to a much larger degree than the $w = 1$ or $w = 2$ prior fits differ from each other, they are not wildly different to the Bayesian analyses. The higgs mass distributions look particularly similar. There is a qualitative difference in Fig. 4g,h, where $m_{\tilde{e}_R}$ and $m_{\tilde{\tau}_1} - m_{\chi_1^0}$ have a non-negligible likelihood up to 1 TeV, unlike the posterior probabilities.

Figs. 5a-f show the profile likelihoods of the pull of various observables. We see that $\Omega_{DM}h^2$ shows a negligible difference to the posteriors. This is because the dark matter relic density constraint dominates the fit and determines the shape and volume of the viable parameter space. Most of the profiles are similar to the posteriors in the figure except for Fig. 5e, where the likelihood extends out to much higher values of the branching ratio of $B_s \to \mu\mu$. These values correspond in Fig. 6b to high $\tan\beta$ but low m_0 points. The posteriors for high $BR(B_s \to \mu\mu) \propto 1/{M_{SUSY}}^2$ are suppressed because of the large volumes at high m_0 (and hence at high M_{SUSY}, where $BR(B_s \to \mu\mu)$ approaches the Standard Model limit due to decoupling). In Fig. 5c, we see enhanced statistical fluctuations in the upper tail of the profile likelihood of M_W, presumably due to a small number of sampled points there. These fluctuations could be reduced with further running of the MCMCs, however.

6. LHC SUSY Cross Sections

In order to calculate pdfs for the expected CMSSM SUSY production cross-sections at the LHC, we use `HERWIG6.500` [59] with the default parton distribution functions. We calculate the total cross-section of the production of two sparticles with transverse momentum $p_T > 100$ GeV. We take the fitted probability distributions of the previous section with the REWSB+same order priors and use `HERWIG6.500` to calculate cross-sections for (a) strong SUSY production i.e. squark and gluino production, (b) inclusive weak gaugino production (i.e. a neutralino or chargino in association with another neutralino, a chargino, a gluino, a squark or a gluino) and (c) 2-slepton production. No attempt is made here to fold in experimental efficiencies or the branching ratios which follow the decays into final state products. The total cross-section times assumed integrated luminosity therefore serves as an upper-bound on the number of events expected at the LHC in the different channels (a)-(c). Some analyses give a few percent for efficiencies, but for specific cases of more difficult signatures, the efficiencies can be tiny.

We show the one dimensional pdfs for the various SUSY production cross-sections in Fig. 7a. We should bear in mind that the LHC is expected to deliver 10 fb^{-1} of luminosity per year in "low-luminosity" mode, whereas afterward this will increase to 30 fb^{-1}. Several years running at $\log_{10}\sigma/\text{fb}= 0$ therefore corresponds to of order a hundred production events for 100 fb^{-1}. $\log_{10}\sigma/\text{fb}= 0$ then gives some kind of rough limit for what might be observable at the LHC, once experimental efficiencies and acceptances are factored in. Luckily, we see that strong production and inclusive weak gaugino production are always above this limit, providing the optimistic conclusion that SUSY will be discovered at the LHC (provided, as always in the present paper, that the CMSSM hypothesis is correct and that the reader accepts our proposal for the prior pdfs). The 95% lower limits on the total direct production cross-sections are 360 fb, 90 fb and 0.01 fb for strongly interacting sparticle, inclusive weak gaugino and slepton production respectively. There therefore is a small chance that direct slepton production may not be at observable rates. The posterior probability that $\sigma(pp \to \tilde{l}^+\tilde{l}^-) < 1$ fb is 0.063. Even in the event that direct slepton production is at too slow a rate to be observable, it is possible that sleptons can be observed and measured by the decays of other particles into them [60]. The pdfs of total SUSY production cross-sections for $w = 2$ are almost identical to those shown in the figure. The main difference is in the total direct slepton production cross section, where the small bump at $\sigma \sim 10^{-2}$ fb is somewhat enlarged. It has the effect of placing the 95% lower bound on the slepton production cross-section at 4.8×10^{-4} fb. For $w = 2$, the chance of the di-slepton production cross-section being less than 1 fb is 0.15. The strong and weak gaugino production cross-sections have 95% lower bounds of 570,90 fb respectively for $w = 2$.

We examine correlations between the various different cross-sections in Figs. 7b-

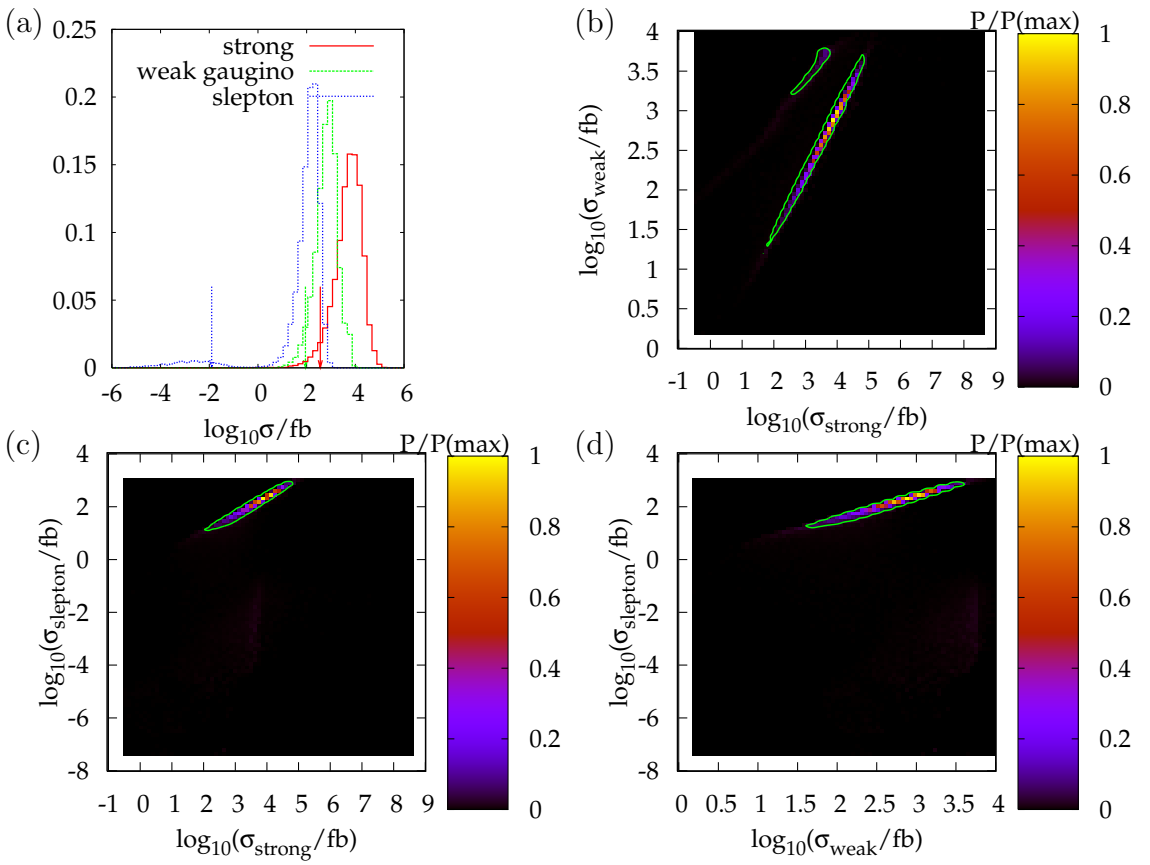

Figure 7: Total SUSY LHC production cross-section pdfs in the CMSSM with REWSB+same order $w = 1$ priors. "strong" refers to squark/gluino production, "weak" to inclusive weak gaugino production and "slepton" to direct slepton production. In (a), 95% *lower* limits on the cross-sections are shown by the vertical arrows. The probability normalised to the bin with maximum probability, is shown by reference to the colour-bar on the right hand side for (b), (c) and (d). The contours show the 95% limits in the two-dimensional plane.

d. For instance, Fig. 7b has two distinct maxima, the focus-point region on the left-hand side and the stau co-annihilation region on the right-hand side. If one could obtain empirical estimates of the total cross-sections to within a factor of about 3 (corresponding to an error of about 0.5 in the $\log_{10}$ value) then measurements of $\sigma_{\rm strong}$ and $\sigma_{\rm weak}$ could distinguish between the two mechanisms. There is a overlap between the one-dimensional projections of the two different regions in either $\sigma_{\rm strong}$ or $\sigma_{\rm weak}$ and so measurements of both seem to be required for discrimination. The probability density of the focus-point region becomes too smeared in the $\sigma_{\rm slepton}$ direction to appear in the 95% limit bounds in Fig. 7c,d. Experimental measurements of the cross-sections in Fig. 7 would provide a test of the CMSSM hypothesis. It is clear from Fig. 7a that $\sigma_{\rm slepton}$ has two isolated probability maxima. The one at

$\sigma_{\rm slepton} < 0$ corresponds to the focus point region, where scalar x masses are large. This region will probably directly produce too few sleptons to be observed at the LHC and so will not be useful there for discriminating the CMSSM focus point region from the co-annihilation region unless there is a significant luminosity upgrade [61].

The profile likelihoods of SUSY production cross-sections are shown in Fig. 8. In the figure, "strong" refers to squark/gluino production, "weak" to inclusive weak gaugino production and "slepton" to direct slepton production. By comparison to fig. 7a, we see that the profile likelihoods generally prefer somewhat larger SUSY production cross-sections than the Bayesian analysis with REWSB+same order $w = 1$ priors. The 95% one-sided lower confidence level bounds upon them are for 2000 fb for sparton production, 300 fb for weak gaugino production and 80 fb for slepton production. This last bound is particularly different from the Bayesian analysis since there the small probability for the focus-point régime, evidenced by the low bump to the left hand side of Fig. 7a, was only pushed just above an integrated posterior pdfs of 5% by volume effects.

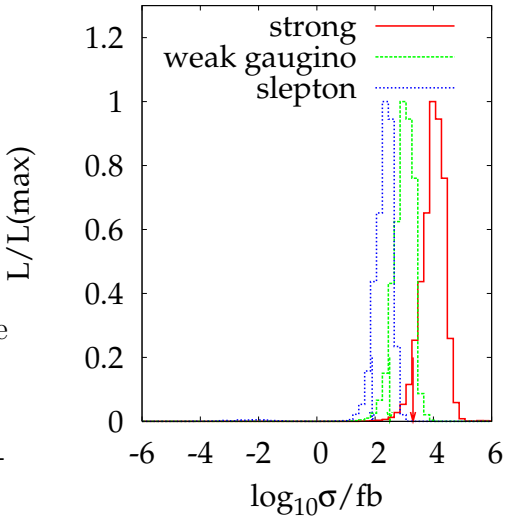

Figure 8: SUSY production cross-section profile likelihoods. One-sided 95% lower confidence level limits are shown as calculated from these histograms by the vertical arrows.

7. Conclusion

This analysis constitutes the first use in a serious physics context of a new "banked" MCMC proposal function [45]. This new proposal function has allowed us to sample simultaneously, efficiently and correctly from both signs of μ. The resulting sampling passed convergence tests and therefore gave reliable estimates of LHC SUSY cross-section pdfs. MCMCs have also been used to determine the impact of potential future collider data upon the MSSM [62, 63, 13]. The development of tools such as the banked proposal MCMC constitutes a goal at least as important as the interesting physics results derived here. In case they may be of use for future work, we have placed the samples obtained by the banked MCMC on the internet, with instructions on how to read them, at the following URL:

`http://users.hepforge.org/~allanach/benchmarks/kismet.html`

We argued that prior probability distributions that are flat in $\tan\beta$ are less natural than those that are flat in the more fundamental Higgs potential parameters μ,

B of the MSSM. We have derived a more natural prior distribution in the form of Eq. 2.8, which is originally flat in μ, B and also encodes our prejudice that μ and the SUSY breaking parameters are "of the same order". There is actually a marginalisation over a family of priors, and as such our analysis uses a hierarchical Bayesian prior distribution. It should be noted that this prior pdf can replace definitions of fine-tuning in the MSSM Higgs sector. Its use in Bayesian statistics is well-defined, and we have examined its effect on Bayesian CMSSM analysis. The main effect is to strongly disfavour the Higgs-pole and focus point dark matter annihilation regions of CMSSM parameter space. The sparticle masses are then predicted to be probably lighter than previously thought as a result of the new prior. There is little difference in the results when one changes the widths of the same order pdfs, but the results are very different to previous ones in the literature where flat priors in $\tan\beta$ were examined. If one rejects the prior flat in the SUSY breaking parameters, as we have advocated here, our results appear rather robust with respect to changes in the prior. However, for readers that find the same order priors too strong, one can view the difference between the flat prior results and those using the same order priors as a result of uncertainty originating from scarce data. This dependence upon priors does indicate the need for caution when interpreting our results; constraining data are currently too scarce to render the posterior pdfs approximately independent of the prior assumption. We feel that the sensitivity to priors must be studied, and find the large dependence on priors consistent with something that is intuitively obvious [64]; that a few pieces of indirect data are not sufficient to robustly constrain a complex model of 8 parameters. The frequentist analysis does not depend on any prior, but it also does not allow us to inject reasonable assumptions about the naturalness of the theory. A comparison between the likelihood profile and posteriors is ideal because it contains information about volume effects in the Bayesian analyses. The frequentist confidence levels on MSSM particle masses are different to Bayesian credible intervals, but within the same ball-park as each other. Thus we may infer some rough limits, but to be conservative one might take the *least constraining* upper bound by any of the different methods. The lighter sparticles from the new priors result in more optimistic total SUSY cross-section predictions for the LHC. It would be interesting to see the footprints of other SUSY breaking models to see whether the correlations between different cross-sections are a good discriminator [65].

A. Comparison With Previous Literature

The flat-prior results may at first sight seem to be in contradiction with the analysis of Ellis *et al* [7], where a preference for light SUSY was found from quite similar global fits to those in the present paper. They also fit $M_W, \sin^2\theta_w^l(\text{eff})$ as well as $(g-2)_\mu$, while using the relic density of dark matter as a constraint. In their paper, Ellis *et al* fixed $\tan\beta$, and all Standard Model inputs at their central experimental values. For

every value of $M_{1/2}$, A_0 scanned, m_0 is adjusted until the central WMAP3 value of $\Omega_{DM}h^2$ results. The smearing due to the finite error on $\Omega_{DM}h^2$ is very small and so it is argued that this procedure well approximates the full constraints upon parameter space. We display the resulting constraint on the $A_0 - M_{1/2}$ plane for $\tan\beta = 10$ and $\mu > 0$ in Fig. 9a. The partial ellipses show the authors' claimed 68% and 90% confidence level limits calculated with $\Delta\chi^2 = 2.30, 4.61$ [7] from the best-fit point, marked by a cross. Actually, since the confidence level regions are constrained within a wedge-shape in the figure, the 68% (90%) limits should not necessarily correspond to $\Delta\chi^2 = 2.30(4.61)$ respectively. The regions shown on the figure should therefore be re-calculated, by calculating what sort of probability distribution $\Delta\chi^2$ has when trapped in such a wedge.

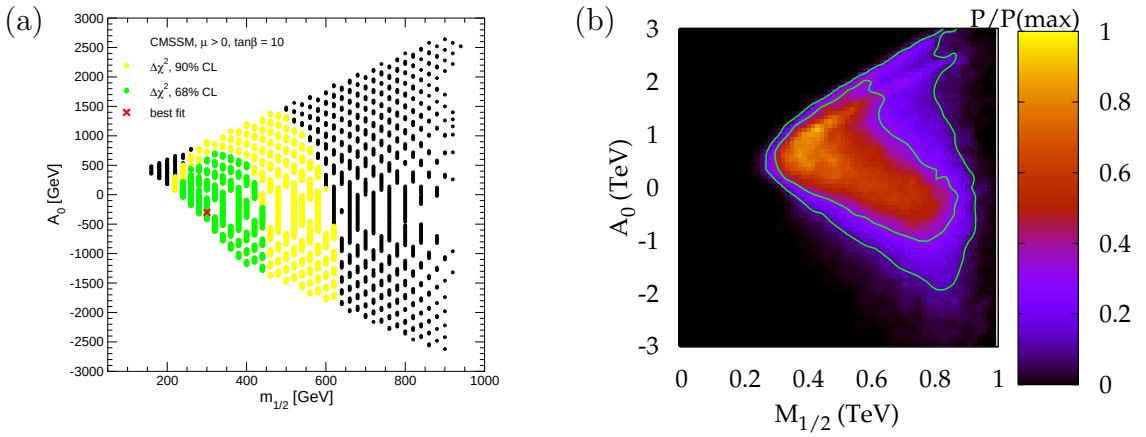

Figure 9: (a) Reduced parameter space global fit from Ref. [7] for $\tan\beta = 10$, $\mu > 0$. In the plot, A_0 has a relative minus sign with respect to the definition used in the present paper, (b) our version of the same fit, marginalised over m_0. 68% and 90% confidence level regions are shown.

In order to emulate these results, we perform a similar but Bayesian analysis with the MCMC algorithm: all Standard Model inputs are fixed at their central empirical values, $\tan\beta = 10$ is fixed and m_0, A_0, $M_{1/2}$ are allowed to vary in the MCMC algorithm in order to fit the combined posterior probability of dark matter plus other measurements. For this comparison, we choose flat priors in $m_0 < 1$ TeV, $M_{1/2} < 1$ TeV and -3 TeV$< A_0 <$3 TeV. The likelihood is calculated as in section 3. The main conclusion from Fig. 9 is that the two results are similar. If the correct relationship between $\Delta\chi^2$ and confidence-level were used in Fig. 9a, the confidence level region could extend out to higher values of $M_{1/2}$. We should note strictly that, being Bayesian confidence regions as compared to frequentist, we do not *exactly* compare like with like in Figs. 9a,b but we do expect roughly similar

confidence regions in the two cases. When we perform a similar fit with a larger allowed range of $m_0 < 4$ TeV, Fig. 9b deforms due to contributions from h^0 and fixed-point regions but the preference for $M_{1/2} < 800$ GeV remains. We conclude from this that Ellis *et al* did not scan larger values of m_0 where the focus point regime resides. The procedure of Ellis *et al* is not suited for including the h^0 and fixed-point regions, since then there is no unique solution of m_0 which provides the central value of $\Omega_{DM}h^2$. If we then additionally include smearing due to $\tan\beta$ in Fig. 9b with a flat prior, the A^0-pole region extends the region of valid $M_{1/2}$ out to higher values > 1 TeV. Allowing variations of Standard Model input parameters produces further smearing in the fits until, finally, Fig. 3a is obtained.

Acknowledgments

This work has been partially supported by STFC. We thank R Rattazzi for discussions which lead to the re-examination of priors. We also thank the Cambridge SUSY working group and T Plehn for helpful discussions and observations. The computational work has been performed using the Cambridge eScience CAMGRID computing facility, with the invaluable help of M Calleja.

References

[1] R. Arnowitt, A. Chamseddine and P. Nath, *Locally supersymmetric grand unification*, Phys. Rev. Lett. **49** (1982) 970;

[2] R. G. Roberts and L. Roszkowski, *Implications for minimal supersymmetry from grand unification and the neutrino relic abundance*, Phys. Lett. B **309** (1993) 329 [arXiv:hep-ph/9301267].

[3] G. L. Kane, C. F. Kolda, L. Roszkowski and J. D. Wells, *Study of constrained minimal supersymmetry*, Phys. Rev. **D49**19946173 [hep-ph/9312272].

[4] J. R. Ellis, K. A. Olive, Y. Santoso and V. C. Spanos, *Likelihood analysis of the CMSSM parameter space*, Phys. Rev. D **69** (2004) 095004 [arXiv:hep-ph/0310356].

[5] S. Profumo and C. E. Yaguna, *A statistical analysis of supersymmetric dark matter in the MSSM after WMAP*, Phys. Rev. D **70** (2004) 095004 [arXiv:hep-ph/0407036].

[6] E. A. Baltz and P. Gondolo, *Markov chain Monte Carlo exploration of minimal supergravity with implications for dark matter*, JHEP **0410** (2004) 052 [arXiv:hep-ph/0407039].

[7] J. R. Ellis, S. Heinemeyer, K. A. Olive and G. Weiglein, *Indirect sensitivities to the scale of supersymmetry*, JHEP **0502** (2005) 013 [arXiv:hep-ph/0411216].

[8] L. S. Stark, P. Hafliger, A. Biland and F. Pauss, *New allowed mSUGRA parameter space from variations of the trilinear scalar coupling A0*, JHEP **0508** (2005) 059 [arXiv:hep-ph/0502197].

[9] J. P. Conlon and F. Quevedo, *Gaugino and scalar masses in the landscape*, JHEP **0606** (2006) 029 [arXiv:hep-th/0605141]; L. E. Ibanez, *The fluxed MSSM*, Phys. Rev. D **71** (2005) 055005 [arXiv:hep-ph/0408064]; A. Brignole, L. E. Ibanez and C. Munoz, *Towards a theory of soft terms for the supersymmetric Standard Model*, Nucl. Phys. B **422** (1994) 125, Erratum-ibid. B **436** (1995) 747 [arXiv:hep-ph/9308271].

[10] B. C. Allanach and C. G. Lester, *Multi-dimensional mSUGRA likelihood maps*, Phys. Rev. D **73** (2006) 015013 [arXiv:hep-ph/0507283].

[11] R. R. de Austri, R. Trotta and L. Roszkowski, *A Markov chain Monte Carlo analysis of the CMSSM*, JHEP **0605** (2006) 002 [arXiv:hep-ph/0602028].

[12] B. C. Allanach, C. G. Lester and A. M. Weber, *The dark side of mSUGRA*, JHEP **12** (2006) 065 [arXiv:hep-ph/0609295]

[13] L. Roszkowski, R. R. de Austri and R. Trotta, *On the detectability of the CMSSM light Higgs boson at the Tevatron*, arXiv:hep-ph/0611173.

[14] B. C. Allanach, *Naturalness priors and fits to the constrained minimal supersymmetric standard model*, Phys. Lett. B **635** (2006) 123 [arXiv:hep-ph/0601089].

[15] G. F. Giudice and R. Rattazzi, *Living dangerously with low-energy supersymmetry*, Nucl. Phys. B **757** (2006) 19 [arXiv:hep-ph/0606105].

[16] D. M. Pierce, J. A. Bagger, K. T. Matchev and R.-J. Zhang, *Precision corrections in the minimal supersymmetric standard model*, Nucl. Phys. B **491** (1997) 3, [arXiv:hep-ph/9606211].

[17] W.-M. Yao *et al*, *The review of particle physics*, Jnl. Phys. **G33** (2006) 1, http://pdg.lbl.gov/

[18] G. F. Giudice and A. Masiero, *A natural solution to the μ problem in supergravity theories*, Phys. Lett. B **206** (1988) 480.

[19] G. E. P. Box and G. C. Tiao, *Bayesian inference in statistical analysis*, Addison Wesley (1973).

[20] B. C. Allanach *et al.*, *The Snowmass points and slopes: Benchmarks for SUSY searches*, in *Proc. of the APS/DPF/DPB Summer Study on the Future of Particle Physics (Snowmass 2001)* ed. N. Graf, *In the Proceedings of APS / DPF / DPB Summer Study on the Future of Particle Physics (Snowmass 2001), Snowmass, Colorado, 30 Jun - 21 Jul 2001, pp P125* [arXiv:hep-ph/0202233].

[21] The Tevatron Electroweak Working Group, *Combination of CDF and D0 results on the mass of the top quark*, [arXiv:hep-ex/0608032].

[22] The Tevatron Electroweak Working Group, *A combination of CDF and D0 results on the mass of the top quark*, [arXiv:hep-ex/0703034].

[23] N. Metropolis, A.W. Rosenbluth, M.N. Teller and E. Teller, *Equations of State Calculations by Fast Computing Machines*, Journal of Chemical Physics, **21** (1953) 1087-1091

[24] D. MacKay, *Information Theory, Inference, and Learning Algorithms*. Cambridge University Press, 2003.

[25] A. E. Nelson and L. Randall, *Naturally large* $\tan\beta$, Phys. Lett. B **316** (1993) 516 [arXiv:hep-ph/9308277]; R. Rattazzi and U. Sarid, *The unified minimal supersymmetric model with large yukawa couplings*, Phys. Rev. D **66** (2002) 010001 [arXiv:hep-ph/9505428].

[26] R. Barbieri and G. F. Giudice, *Upper bounds on supersymmetric particle masses*, Nucl. Phys. B **306** (1988) 63; B. de Carlos and J. A. Casas, *One loop analysis of the electroweak breaking in supersymmetric models and the fine tuning problem*, Phys. Lett. B **309** (1993) 320, [arXiv:hep-ph/9303291]; R. Barbieri and A. Strumia, *About the fine-tuning price of LEP*, Phys. Lett. B **433** (1998) 63, [arXiv:hep-ph/9801353]; C. Giusti, A. Romanano and A. Strumia. *Natural ranges of supersymmetric signals*, Nucl. Phys. B **550**, 3 (1999) [arXiv:hep-ph/9811386]; L. E. Ibanez and G. G. Ross, *Supersymmetric Higgs and radiative electroweak breaking*, arXiv:hep-ph/0702046.

[27] B.C. Allanach, *SOFTSUSY: A program for calculating supersymmetric spectra*, Comput. Phys. Commun. **143** (2002) 305, [arXiv:hep-ph/0104145].

[28] P. Skands *et al*, *SUSY Les Houches accord: Interfacing SUSY spectrum calculators, decay packages, and event generators*, JHEP **0407** (2004) 036, [arXiv:hep-ph/0311123].

[29] G. Bélanger, F. Boudjema, A. Pukhov and A. Semenov, *micrOMEGAs: Version 1.3*, Comput. Phys. Commun. **174** (2006) 577 [arXiv:hep-ph/0405253]; G. Bélanger, F. Boudjema, A. Pukhov and A. Semenov, *micrOMEGAs: A program for calculating the relic density in the MSSM*, Comput. Phys. Commun. **149** (2002) 103 [arXiv:hep-ph/0112278].

[30] G.W. Bennett *et al.* [Muon g-2 collaboration], *Final report of the muon E821 anomalous magnetic moment measurement at BNL*, Phys. Rev. D **73** (2006) 072003 [arXiv:hep-ex/0602035].

[31] K. Hagiwara, A.D. Martin, D. Nomura, and T. Teubner, *Improved predictions for g-2 of the muon and alpha(QED)(M(Z)**2)*, (2006) [arXiv:hep-ph/0611102].

[32] M. Passera, *Precise mass-dependent QED contributions to leptonic g-2 at order alpha**2 and alpha**3*, Phys. Rev. D **75** (2007) 013002, [arXiv:hep-ph/0606174].

[33] A. Czarnecki, W.J. Marciano, and A. Vainshtein, *Refinements in electroweak contributions to the muon anomalous magnetic moment*, Phys. Rev. D **67** (2003) 073006 [arXiv:hep-ph/0212229]

[34] U. Chattopadhyay and P. Nath, *Probing supergravity grand unification in the Brookhaven g-2 experiment*, Phys. Rev. D **53** (1996) 1648, [arXiv:hep-ph/9507386].

[35] S. Heinemeyer, D. Stöckinger and G. Weiglein, *Electroweak and supersymmetric two-loop corrections to (g-2)(mu)*, Nucl. Phys. **B690** (2004) 103, [arXiv:hep-ph/0405255]; S. Heinemeyer, D. Stöckinger and G. Weiglein, *Two-loop SUSY corrections to the anomalous magnetic moment of the muon*, Nucl. Phys. B **690** (2004) 62 [arXiv:hep-ph/0312264].

[36] D. Stöckinger, *The muon magnetic moment and supersymmetry*, [arXiv:hep-ph/0609168].

[37] Tevatron Electroweak Working Group & The CDF Collaboration, *Winter 2007 Conference Note*, http://fcdfwww.fnal.gov/physics/ewk/2007/wmass/.

[38] [The ALEPH, DELPHI, L3, OPAL, SLD Collaborations, the LEP Electroweak Working Group, the SLD Electroweak and Heavy Flavour Groups], *Precision electroweak measurements on the Z resonance*, Phys. Rept. **427** (2006) 257 [arXiv:hep-ex/0509008]; [The ALEPH, DELPHI, L3 and OPAL Collaborations, the LEP Electroweak Working Group], *A combination of preliminary electroweak measurements and constraints on the standard model*, [arXiv:hep-ex/0511027].

[39] M. Awramik, M. Czakon, A. Freitas, and G. Weiglein, *Precise prediction for the W-boson mass in the standard model*, Phys. Rev. D **69** (2004) 053006 [arXiv:hep-ph/0311148].

[40] The code is forthcoming in a publication by A. M. Weber et al.; S. Heinemeyer, W. Hollik, D. Stöckinger, A. M. Weber and G. Weiglein, *Precise prediction for M(W) in the MSSM*, JHEP **08** (2006) 052, [arXiv:hep-ph/0604147].

[41] J. Haestier, S. Heinemeyer, D. Stöckinger and G. Weiglein, *Electroweak precision observables: Two-loop Yukawa corrections of supersymmetric particles*, *JHEP* **0512** (2005) 027, [arXiv:hep-ph/0508139].

[42] E. Barberio *et al* [Heavy Flavour Averaging Group], *Averages of b-hadron Properties at the End of 2005*, arXiv:hep-ex/0603003.

[43] P. Gambino, U. Haisch and M. Misiak, *Determining the sign of the $b \to s\gamma$ amplitude*, Phys. Rev. Lett. **94** (2005) 061803 [arXiv:hep-ph/0410155].

[44] D. N. Spergel *et al.*, *Wilkinson Microwave Anisotropy Probe (WMAP) three year results Implications for cosmology*, arXiv:astro-ph/0603449.

[45] B. C. Allanach and C. G. Lester, *Sampling using a 'bank' of clues*, arXiv:0705.0486 [hep-ph]

[46] see, for example, section 7.3 of F. James, *Minuit, function minimization and error analysis*, CERN Program Library Long Writeup D506.

[47] A. J. Barr, *Using lepton charge asymmetry to investigate the spin of supersymmetric particles at the LHC*, Phys. Lett. B **596** (2004) 205 [arXiv:hep-ph/0405052].

[48] A. Gelman and D. Rubin, *Inference from Iterative Simulation Using Multiple Sequences*, Stat. Sci. **7** (1992) 457.

[49] K. Griest and D. Seckel, *Three exceptions in the calculation of relic abundances*, Phys. Rev. **D43** (1991) 3191–3203.

[50] M. Drees and M. M. Nojiri, *The Neutralino Relic Density in Minimal N=1 Supergravity*, Phys. Rev. **D47** (1993) 376–408, [arXiv:hep-ph/9207234].

[51] R. Arnowitt and P. Nath, *Cosmological Constraints and SU(5) Supergravity Grand Unification*, Phys. Lett. **B299** (1993) 58–63, [arXiv:hep-ph/9302317].

[52] A. Djouadi, M. Drees and J. L. Kneur, *Neutralino dark matter in mSUGRA: Reopening the light Higgs pole window,*, Phys. Lett. B **624** (2005) 60 [arXiv:hep-ph/0504090].

[53] K. L. Chan, U. Chattopadhyay and P. Nath, *Naturalness, Weak Scale Supersymmetry and the Prospect for the Observation of Supersymmetry at the Tevatron and at the LHC*, Phys. Rev. **D5** (1998) 096004, [arXiv:hep-ph/9710473]; A. B. Lahanas, N. E. Mavromatos and D. V. Nanopoulos, *WMAPing the universe: Supersymmetry, dark matter, dark energy, proton decay and collider physics*, Int. J. Mod. Phys. D **12**, 1529 (2003) [arXiv:hep-ph/0308251]; U. Chattopadhyay, A. Corsetti and P. Nath, *WMAP constraints, SUSY dark matter and implications for the direct detection of SUSY*, Phys. Rev. D **68**, 035005 (2003) [arXiv:hep-ph/0303201].

[54] J. L. Feng, K. T. Matchev, and T. Moroi, *Multi-TeV scalars are natural in minimal supergravity*, Phys. Rev. Lett. **84** (2000) 2322–2325, [arXiv:hep-ph/9908309].

[55] J. L. Feng, K. T. Matchev, and T. Moroi, *Focus points and naturalness in supersymmetry*, Phys. Rev. **D61** (2000) 075005, [arXiv:hep-ph/9909334].

[56] J. L. Feng, K. T. Matchev, and F. Wilczek, *Neutralino dark matter in focus point supersymmetry*, Phys. Lett. **B482** (2000) 388–399, [arXiv:hep-ph/0004043];

[57] R. Arnowitt *et al.*, *Measuring the stau - neutralino(1) mass difference in co-annihilation scenarios at the LHC*, arXiv:hep-ph/0608193.

[58] S. S. Wilks, *The large-sample distribution of the likelihood ratio for testing composite hypotheses*, Ann. Math. Statist. 9, **60** (1938) 95.

[59] G. Corcella *et al*, *HERWIG 6: an event generator for hadron emission reactions with intefering gluons (including supersymmetric processes)*, JHEP **0101** (2001) 010 [arXiv:hep-ph/0011363]; *ibid.*, *HERWIG 6.5 release note*, arXiv:hep-ph/0210213; S. Moretti, K. Odagiri, P. Richardson, M.H. Seymour and B.R. Webber, *Implementation of supersymmetric processes in the HERWIG event generator*, JHEP 0204 (2002) 028 [hep-ph/0204123].

[60] B. C. Allanach, C. G. Lester, M. A. Parker and B. R. Webber, *Measuring sparticle masses in non-universal string inspired models at the LHC*, JHEP **0009** (2000) 004 [arXiv:hep-ph/0007009].

[61] F. Gianotti *et al.*, *Physics potential and experimental challenges of the LHC luminosity upgrade*, Eur. Phys. J. C **39** (2005) 293 [arXiv:hep-ph/0204087].

[62] C. G. Lester, M. A. Parker and M. J. White, *Determining SUSY model parameters and masses at the LHC using cross-sections, kinematic edges and other observables*, JHEP **0601** (2006) 080 [arXiv:hep-ph/0508143].

[63] E. A. Baltz, M. Battaglia, M. E. Peskin and T. Wizansky, *Determination of dark matter properties at high-energy colliders*, Phys. Rev. D **74** (2006) 103521 [arXiv:hep-ph/0602187].

[64] M. Goldstein, proceedings of Advanced Statistical Techniques in Particle Physics, Durham (2002), URL http://www.ippp.dur.ac.uk/Workshops/02/statistics/proceedings.shtml

[65] B. C. Allanach, D. Grellscheid, F. Quevedo, *Genetic Algorithms and Experimental Discrimination of SUSY Models*, JHEP **07** (2004) 069 [arXiv:hep-ph/0406277]; J. L. Bourjaily, G. L. Kane, P. Kumar and T. T. Wang, *Outside the mSUGRA box*, arXiv:hep-ph/0504170; N. Arkani-Hamed, G. L. Kane, J. Thaler and L. T. Wang, *Supersymmetry and the LHC inverse problem*, JHEP **0608** (2006) 070 [arXiv:hep-ph/0512190]; G. L. Kane, P. Kumar and J. Shao, *LHC string phenomenology*, arXiv:hep-ph/0610038. J. Conlon, S. Kom, K. Suraliz, B. C. Allanach and F. Quevedo, *Supersymmetric particle spectra and LHC collider phenomenology for large volume string models*, arXiv:0704.3403 [hep-ph].